Interfacial Reactions between Sn–Ag Lead-Free Solders and Polycrystalline and Single-Crystal Copper

Jing Han [a, *], Hongjin Zhou [a], Zixuan Li [a], Chenxi Zhao [a], Zhenya Zhang [b], Guangming Zhang [c], Fu Guo [a, d]

[a] College of Materials Science and Engineering, Beijing University of Technology, Beijing 100124, China

[b] Key Laboratory of Green Fabrication and Surface Technology of Advanced Metal Materials (Anhui University of Technology), Ministry of Education, Ma'anshan 243002, PR China

[c] General Engineering Research Institute, School of Engineering and Built Environment, Faculty of Health, Innovation, Technology and Science, Liverpool John Moores University, Liverpool, L3 3AF, UK

[d] Beijing Information Science & Technology University, China

Abstract

With the trend of solder joint miniaturization, the proportion of interfacial intermetallic compounds in the overall solder joint structure has increased, making interfacial reactions and microstructures key factors that restrict solder joint performance. As a widely used pad material in electronic packaging, the grain boundaries of polycrystalline copper can interfere with the accurate analysis of interfacial reaction laws. In contrast, single-crystal copper can effectively eliminate grain-boundary interference and reveal the intrinsic growth law of interfacial intermetallic compounds (IMC), thereby possessing irreplaceable value in research on micro-solder joint reliability.

Based on this, this study investigates the interfacial reactions during the reflow process and subsequent aging reactions of two solders, namely Sn3.5Ag0.5Bi8In and Sn3Ag0.5Cu, on polycrystalline copper and single-crystal copper with (001) and (111) orientations, respectively, at 260 °C and 285 °C. By investigating the morphological evolution and growth behavior of interfacial IMCs on pads with different orientations and combining comparative analysis, the influence mechanism of polycrystalline copper/single-crystal copper pads on the morphological evolution and growth behavior of IMCs at the Sn-Ag series solder/Cu interface is revealed.

Key words: Lead-free solder; Single crystal copper; Interface reaction; Aging process

1. Introduction

In the field of microelectronic manufacturing, electronic packaging technology plays an increasingly critical role. It has shifted from relying on electronic systems and integrated circuit technologies to developing in synchronization with them, aiming to address various challenges faced by electronic devices and products in their pursuit of high performance, miniaturization, and multi-functionality.

Electronic packaging technology is a key factor affecting chip size. With the continuous advancement of electronic packaging technology, the requirements for high reliability, high density, and miniaturization of packaging across various fields are continually increasing [1]. This demand has also raised requirements for the solder joint dimensions, resulting in a significant reduction in interconnect sizes and a marked increase in integration density. Furthermore, in terms of electrical interconnects, miniaturized solder joints can significantly enhance interconnect performance, thereby better meeting the packaging needs of electronic products. Currently, the miniaturization of solder joints has become a mainstream trend[2]; the proportion of interfacial intermetallic compounds in the overall solder joint structure has increased[3], and interfacial

* Corresponding author.
E-mail address: hanjing@bjut.edu.cn (J. Han)

reactions and microstructures have emerged as key factors limiting solder joint performance.

In the electronic packaging process, Cu is often used as a material for pads and substrates due to its excellent electrical and thermal conductivity[4]. In solder joints, Cu-Sn intermetallic compounds (IMCs) are among the most important intermetallic compounds[5-7], playing a critical role in solder joint performance. Furthermore, as packaging density increases and pad size shrinks, polycrystalline copper exhibits abundant randomly distributed grain boundaries. These grain boundaries can interfere with the accurate analysis of interfacial reaction laws, making it difficult to elucidate the intrinsic growth behavior of IMCs. In contrast, single-crystal copper, free of grain boundaries, eliminates the complex effects of grain boundaries on atomic diffusion and the nucleation and growth of IMC. This makes it more conducive to exploring the intrinsic laws of interfacial reactions. Therefore, single-crystal copper is often used as the research object in relevant studies to avoid interference factors in polycrystalline copper studies, thereby enabling accurate analysis of the interfacial interaction mechanism between solder and copper substrates. Accordingly, it is essential to investigate the interfacial reaction between single-crystal copper and solder[8].

Domestic and international research on this topic mainly focuses on two aspects: first, comparative studies between single-crystal copper and polycrystalline copper, specifically analyzing the influence of single-crystal copper on the morphological evolution of IMC formed at the interface; second, research on orientation relationships, specifically involving Cu_3Sn/single-crystal copper, solder/Cu_6Sn_5, Cu_6Sn_5/single-crystal copper, and Cu_6Sn_5/Cu-Sn[9-11] Although single-crystal copper offers remarkable advantages for eliminating grain-boundary interference and revealing the intrinsic growth behavior of IMCs, and relevant research has advanced along these two core avenues, existing studies still lack a systematic explanation of the fundamental mechanism of interfacial reactions.

Meanwhile, in microelectronic packaging technology, the requirements for solder reliability and environmental friendliness are continually increasing. Developing lead-free solders to replace traditional Sn-Pb solders has become a key task. This requires new-type solders to possess advantages such as low melting point, good wettability, low cost, non-toxic elements (harmless to the human body), excellent thermal and mechanical properties, and good corrosion resistance. Among them, ternary or quaternary lead-free solders have promising development prospects, especially SnAgCu-based and SnAgBiIn-based solders, which exhibit excellent solderability and electrical conductivity. For example, binary alloys such as near-eutectic Sn-Ag alloys or Sn-3.5Ag eutectic alloys cannot meet packaging needs due to their poor wettability, high cost, and high melting point[12]. However, building on these alloys, incorporating small amounts of third alloying elements such as Bi, Zn, and Cu, or fourth alloying elements with a content of less than 1%, can not only lower the melting point of the solder and reduce costs but also enhance the solder's performance in terms of strength, wettability, and thermal shock reliability[13]. Therefore, based on current research foundations and production processes, Sn-based alloy solders doped with 1-2 additional elements are the most widely used, primarily involving elements such as Bi, In, Cu, and Zn[4,5][14-22]. However, current research on quaternary alloy solders remains limited. There is an urgent need to develop a suitable SnAgBiIn quaternary alloy solder with an appropriate alloying element ratio that can be well applied in practical industrial production.

In this study, polycrystalline copper and single-crystal copper with two orientations [(001) and (111)] were used as pads, and two types of solders (Sn3.5Ag0.5Bi8In and Sn3Ag0.5Cu) were employed. The morphological evolution and growth behavior of IMC on pads with different orientations were investigated during the reflow process and aging reaction. Through comparative analysis, the influence mechanism of polycrystalline copper/single-crystal copper pads on the morphological evolution and growth behavior of IMC at the Sn-Ag series solder/Cu interface was revealed.

2. Sample preparation and testing

2.1 Samples preparation

2.1.1 Materials

Two types of solders, Sn3.5Ag0.5Bi8In (SABI) and Sn3Ag0.5Cu (SAC305), were used in this study, both supplied by the Beijing General Research Institute for Non-Ferrous Metals. The polycrystalline copper sheets had a dimension of 1 mm × 1 mm × 0.5 mm. The single-crystal copper was in the form of blocks with a diameter of 10 mm, with orientations (001) and (111), provided by Hefei Kejing Materials Technology Co, Ltd. These single-crystal copper blocks were cut into 1 mm × 1 mm × 0.5 mm sheets via wire electrical discharge machining (WEDM). The samples were sequentially ground using SiC abrasive papers up to 4000 grit, followed by mechanical polishing with 1 μm diamond paste and 0.3 μm alumina suspension to obtain a mirror-like surface. The polished specimens were then ultrasonically cleaned in ethanol for 5 min to remove residual contaminants, and finally dried with compressed air before further processing.

2.1.2 Preparation of BGA solder balls

The setup used to fabricate BGA solder balls is shown in Fig. 1. The printing plate contained holes with a 400 μm diameter. The solder paste was first printed onto the glass plate using a scraper, and heated to 250℃. After complete melting, the solder was allowed to solidify by cooling to room temperature in air, forming spherical solder balls. After cleaning, the samples were dried and stored in a desiccator for subsequent use.

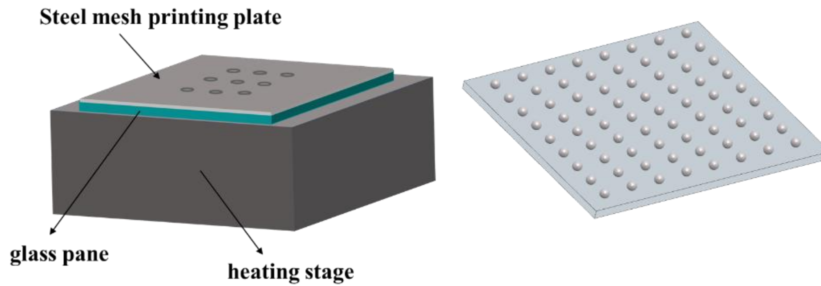

Fig. 1 Platform for BGA solder balls preparation

2.2 Testing method

2.2.1 Reflow

Before soldering, the polished polycrystalline and single-crystal copper substrates (with (001) and (111) orientations) were gently wiped with ethanol-soaked gauze to remove surface contaminants and ensure clean interfaces. Subsequently, a small amount of flux was uniformly applied to the copper surfaces to promote wetting. The reflow experiments were conducted on an ST325 hot-air rework station manufactured by PACE (USA).

The reflow temperature and time are listed in Table. 1. After reflow, the samples were allowed to cool naturally to room temperature in air. The prepared samples were then observed to analyze two aspects: first, the growth behavior of IMC formed at the interfaces between Sn-Ag-based lead-free solders and the pads (polycrystalline copper, (001) single-crystal copper, and (111) single-crystal copper); second, the influence of two lead-free solders with different compositions on the IMC growth behavior during this process.

Table. 1 Sample reaction conditions for different research content

Sample	Solder composition (at.%)	Reaction temperature (°C)	Reaction time (s)
S1	Sn3Ag0.5Cu	260/285	10
S2	Sn3Ag0.5Cu	260/285	60
S3	Sn3Ag0.5Cu	260/285	120
S4	Sn3.5Ag0.5Bi8In	260/285	10
S5	Sn3.5Ag0.5Bi8In	260/285	60
S6	Sn3.5Ag0.5Bi8In	260/285	120

2.2.2 Aging

The soldered convex points were divided into two groups: one for initial morphology observation and the other for the aging experiment.

After reflow, the samples were cooled to room temperature. The solder joints were then placed in an electric constant-temperature drying oven for aging treatment. The aging durations were set to 5, 10, 20, and 40 days, with a fixed temperature of 150 °C. The aged samples were hermetically sealed.

2.2.3 Microstructure Characterization and IMC Thickness Measurement

The interfacial microstructure of the solder joint was observed using scanning electron microscopy (SEM), and the composition of the interfacial IMCs was analyzed by energy-dispersive spectroscopy (EDS).

Before microstructural observation, the solder joint samples were cross-sectioned, embedded in epoxy resin, and subsequently subjected to standard metallographic grinding and polishing to obtain a flat, smooth cross-sectional surface. The thickness of the interfacial IMC layer was measured using image analysis software. For each sample, at least 5 measurement points were selected at different locations along the interface, and the average of these values was taken as the average IMC thickness for that sample.

3. Results and Discussion

3.1 Interfacial Reactions of SAC305 Solder with Polycrystalline Copper and Single-Crystal Copper

The surface morphology of SAC305 solder after reflow with copper pads is shown in Fig. 2. The interfacial IMC formed between SAC305 solder and polycrystalline copper pads exhibits a scalloped morphology, with non-uniform grain sizes and an irregular distribution. The boundaries between adjacent grains are clear and distinct, with small differences. This behavior is attributed to the high density of randomly distributed grain boundaries in polycrystalline copper, which hinders the directional growth of IMC grains. Furthermore, the elevated interfacial energy at grain boundaries, coupled with differences in grain boundary diffusion rates, leads to continuous changes in growth direction during IMC formation, resulting in an irregular, scalloped structure.

On (001)-oriented single-crystal copper, the interfacial IMC exhibits a prismatic morphology. The grains are larger than the surrounding scallop-shaped grains, and the angle between adjacent grains is approximately 90°. This is because (001)-oriented single-crystal copper has no grain boundary interference, and the symmetry of the crystal orientation directly determines the prismatic morphology of the IMC and the 90° angle between grains. Additionally, the atomic arrangement of the (001) crystal plane exhibits two-dimensional orthogonal symmetry. The diffusion rate of Cu atoms along the orthogonal (100) and (010) directions is higher than in other directions, promoting the preferential nucleation and growth of interfacial compounds along these two directions, then leading to the formation of prismatic grains.

Similarly, the IMC formed on a single-crystal copper (111) substrate also exhibits a prismatic morphology. The grain boundaries between adjacent grains are distinctly clear, and the angle between adjacent grains is

approximately 60°. This is because the (111) plane is the close-packed plane of copper and exhibits six-fold symmetry. Cu atoms diffuse most rapidly along the three equivalent directions — (110), (101), and (011) — which are mutually oriented at 60° angles. As a result, IMC growth is guided along these directions, producing prismatic grains with orientations consistent with the substrate's symmetry.

Furthermore, the morphology of the interfacial IMC is not only dependent on the crystallographic orientation of the copper substrate but also intimately linked to the atomic diffusion behavior of the Cu_6Sn_5 phase. In polycrystalline copper, the abundance of grain boundaries provides rapid diffusion pathways for Cu atoms, introducing randomness into IMC growth and resulting in the formation of scallop-shaped grains. In contrast, on a single-crystal copper substrate, owing to the absence of grain-boundary diffusion pathways, the IMC growth is more readily governed by the substrate's crystallographic orientation, leading to the formation of regular, prismatic grains.

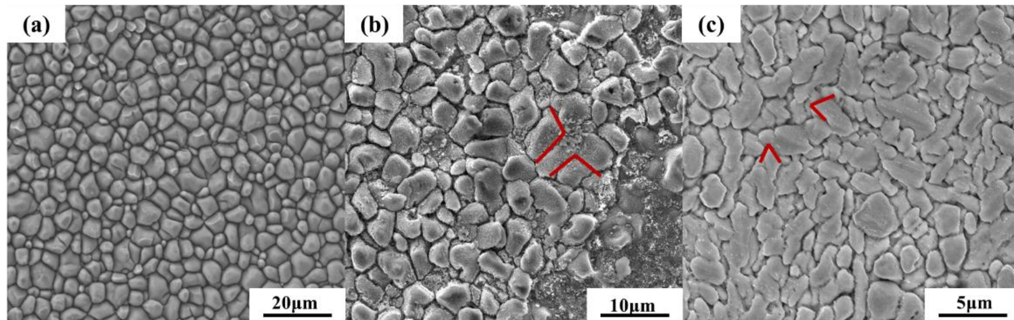

Fig. 2 Top views of Sn3Ag0.5Cu solder joints with polycrystalline copper, (001)-oriented single-crystal copper, and (111)-oriented single-crystal copper after reflow at 260°C for 60s

Fig. 3 and Fig. 4 show the cross-sectional microstructures of interfacial IMCs formed during the reflow soldering of SAC305 on polycrystalline copper and on (001)- and (111)-oriented single-crystal copper at 260°C and 285°C, respectively. It can be observed that, on the polycrystalline copper pads, the interfacial IMCs exhibit a scalloped morphology. With increasing soldering time and temperature, the average thickness of the interfacial Cu_6Sn_5 layer increases continuously. This is because longer reflow times and higher reflow temperatures facilitate the interdiffusion of Cu and Sn atoms, thereby promoting interfacial reactions and accelerating IMC growth. In addition, the high density of grain boundaries in polycrystalline copper provides fast diffusion pathways for Cu atoms, further facilitating the growth of the interfacial IMC layer during reflow.

Unlike the convex point of polycrystalline copper, the cross-sectional IMC at the convex point of (001)-oriented single-crystal copper exhibits a ridged morphology with sharp corners. As the reflow time increases, the height of angular protrusions on the interfacial IMC increases, making the ridged shape more obvious. This behavior is associated with the fixed crystallographic orientation of the single-crystal substrate, which constrains IMC growth along specific directions. As a result, the IMC morphology in cross-section appears as aligned ridges with distinct sharp tips.

Similar to (001)-oriented single-crystal copper, the cross-sectional IMC at the convex point of (111)-oriented single-crystal copper also shows a rod-like morphology with sharp corners. The key difference is that the tip angle of these rod-like grains is larger, approaching 120°. Additionally, as the reflow time increases, the thickness of the interfacial IMC increases, and the ridged characteristics become more distinct. This feature is related to the six-fold symmetry of the (111) plane, which allows IMCs to grow along multiple equivalent crystallographic directions, leading to ridge structures with interfacial angles close to 120°. Furthermore, under identical soldering durations, the average thickness of interfacial Cu_6Sn_5 is greater at 285°C, and the ridge tip angles more closely approach 120°.

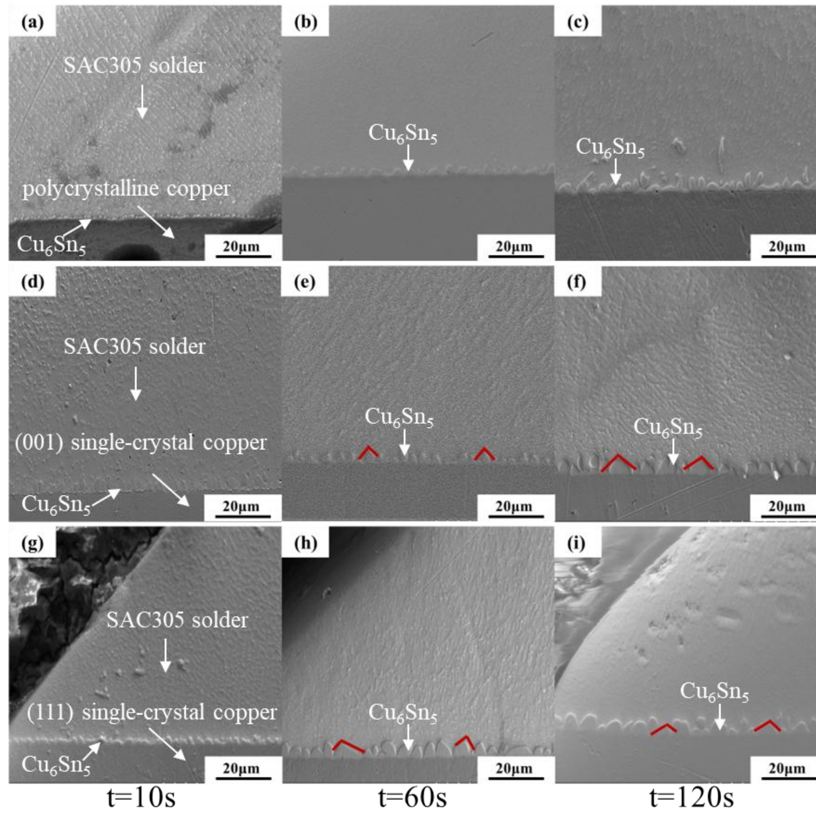

Fig. 3 Cross-sectional morphologies of interfacial intermetallic compounds (IMCs) formed between Sn3Ag0.5Cu solder and polycrystalline copper (a-c), (001) single-crystal copper (d-f), and (111) single-crystal copper (g-i) at 260 ℃ under different reflow times

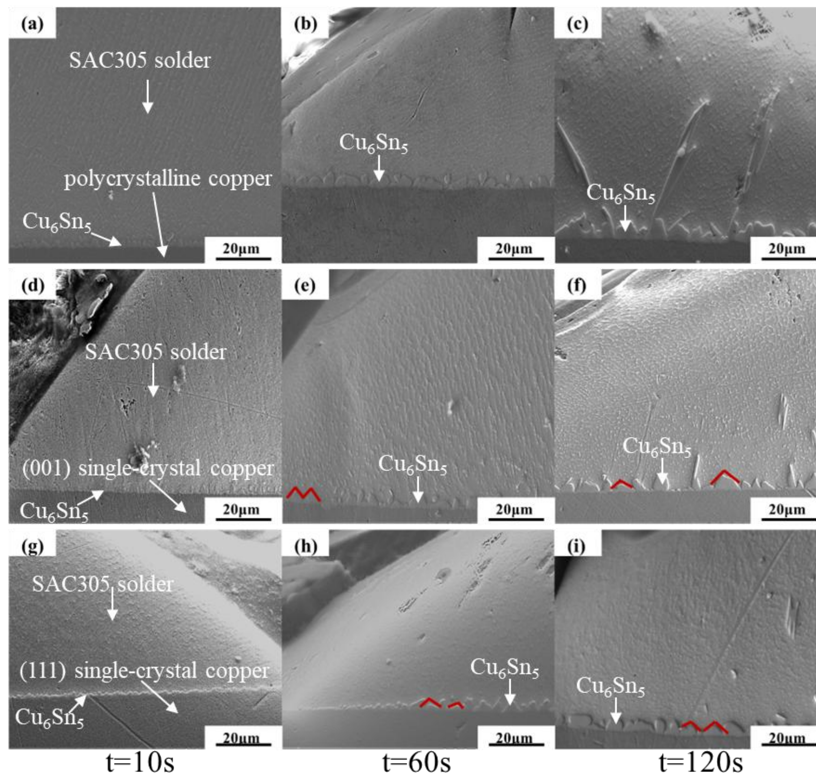

Fig. 4 Cross-sectional morphologies of interfacial intermetallic compounds (IMCs) formed between Sn3Ag0.5Cu solder and polycrystalline copper (a-c), (001) single-crystal copper (d-f), and (111) single-crystal copper (g-i) at 285 ℃ under different reflow times

3.2 Interfacial Reactions of SABI Solder with Polycrystalline Copper and Single-Crystal Copper

Fig. 5 (a)-(c) shows the top-view interfacial morphologies of SABI solder joints reflowed with polycrystalline Cu, (001) single-crystal Cu, and (111) single-crystal Cu substrates at 260°C for 60 s. Compared with SAC305 solder, the Cu_6Sn_5 grains formed during the reflow of SABI solder are smaller and more uniformly distributed. This is because the addition of Bi and In reduces the melting temperature and increases the degree of solidification undercooling. As a result, the nucleation rate is enhanced, providing a larger number of nucleation sites for both the Sn-rich phase and interfacial reaction products, thereby leading to the formation of finer IMC grains. However, the increased nucleation density also introduces slight variability in grain size.

On polycrystalline copper pads, the interfacial IMCs in SABI solder joints exhibit a scalloped morphology with non-uniform grain sizes and irregular distributions, and the grain boundaries between adjacent grains are relatively distinct. On (001)-oriented single-crystal copper pads, the IMCs display a more pronounced prismatic morphology, with relatively uniform grain sizes and a regular arrangement, and the angles between adjacent grains are approximately 90°. A similar prismatic morphology is also observed on (111) single-crystal Cu substrates. This is due to the absence of grain-boundary constraints and the well-defined crystallographic symmetry of single-crystal copper. Consequently, the diffusion rate of Cu atoms along specific symmetry directions is significantly higher than in other directions. Under such conditions, the fine IMC grains in SABI solder tend to grow preferentially along these directions without deviating from their intended trajectories due to growth interference between adjacent grains, thereby promoting the development of well-defined prismatic structures.

Moreover, under identical reflow conditions, distinct differences in the interfacial IMC morphologies formed by different solders on the same copper pad are observed. The intermetallic compounds in SAC305 solder joints exhibit a scalloped morphology, while those in SABI solder joints show a flower-like morphology. To investigate this phenomenon, EPMA analysis was conducted on the interfacial IMCs, as shown in Fig. 5 (d)-(i). The results indicate that the main components of the interfacial IMC are Cu_6Sn_5, Cu_3Sn, and $Ag_3(SnIn)$, with the element distribution as shown in Table. 2, and the flower-like IMC was identified as $Ag_3(SnIn)$. The formation of these flower-like IMCs is closely related to the addition of Bi and In. During reflow, Bi tends to segregate at the interface, suppressing vertical IMC growth while promoting lateral branching. Simultaneously, Bi lowers the interfacial energy between the IMCs and the solder, driving the system toward branched morphologies with larger surface areas. Furthermore, the addition of the In element makes the grain boundary diffusion coefficient of $Ag_3(SnIn)$ less than that of Cu_6Sn_5, suppressing excessive grain coarsening and preserving the fine branched structure, ultimately resulting in the flower-like morphology.

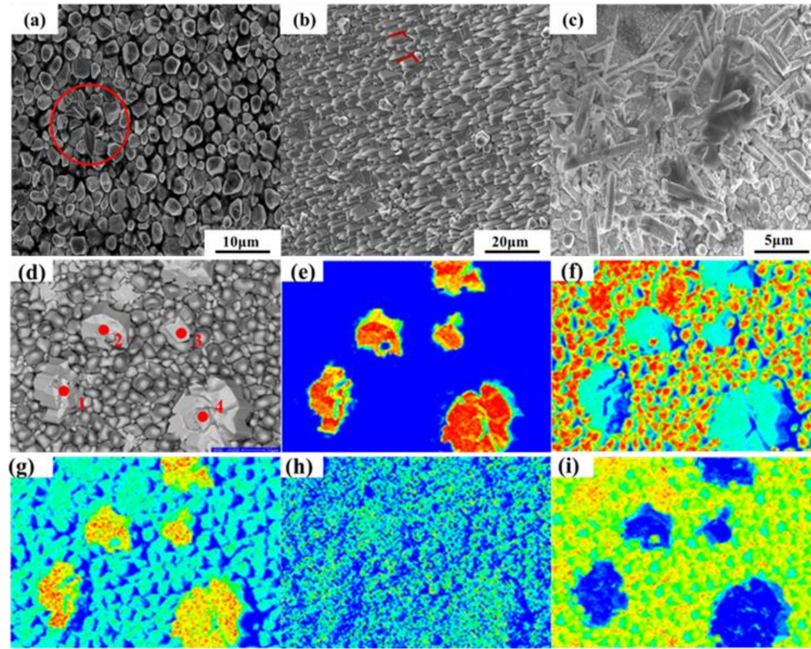

Fig. 5 (a-c) Top-view morphologies of Sn3.5Ag0.5Bi8In solder joints on polycrystalline copper, (001) single-crystal copper, and (111) single-crystal copper substrates after reflow at 260 °C for 60 s; (d) EPMA elemental mapping of the Sn3.5Ag0.5Bi8In/Cu solder joint under the same conditions; (e-i) corresponding elemental distributions of Ag, Sn, In, Bi, and Cu, respectively

Table. 2 Sn3.5Ag0.5Bi8In is welded on polycrystalline copper at 260℃ for 60s, the top view of the solder joint element distribution table

	1	2	3	4
Sn(Mass%)	18.453	19.645	20.284	18.926
Cu(Mass%)	3.65	8.121	4.037	3.459
Ag(Mass%)	71.159	66.266	69.751	71.28
In(Mass%)	6.68	5.849	5.854	6.286
Bi(Mass%)	0.059	0.119	0.074	0.05

Fig. 6 and Fig. 7 show the cross-sectional morphologies of the interfacial IMCs formed between SABI solder and polycrystalline Cu, (001) single-crystal Cu, and (111) single-crystal Cu substrates at 260 °C and 285 °C for different reflow times. On polycrystalline copper pads, compared with SAC305 solder, the interfacial IMC on the convex-point cross-sections formed with SABI solder exhibits a smaller thickness but a larger height variation. This is because the addition of Bi and In promotes the nucleation of Cu_6Sn_5 and refines its grains, ultimately reducing the interfacial IMC thickness. The height of interfacial IMC on the convex-point cross-sections of SABI solder varies greatly. This is attributed to the anisotropy of Cu_6Sn_5: during interfacial IMC growth, grains with different orientations exhibit different surface energies. As the system tends toward a lower Gibbs free energy, grains with higher surface energy become unstable, dissolve, and are swallowed by grains with lower surface energy, thereby increasing size disparity. This effect becomes more evident with increasing reflow time. Additionally, the growth of the IMC layer is mainly controlled by the interdiffusion of Cu and Sn atoms. Increasing the reflow temperature and time significantly accelerates atomic diffusion, thereby promoting the growth of the Cu_6Sn_5 layer. As a result, the IMC layer formed at 285 °C is markedly thicker than that at 260 °C. Meanwhile, the IMC morphology becomes more regular, and the prismatic features become more distinct.

On (001)-oriented single-crystal copper, the interfacial IMC transforms from a scalloped morphology to a

prismatic morphology with increasing reflow time. When the reflow time exceeds a threshold, the interfacial IMC reverts to a scalloped morphology, while the grain size continues to increase. This is because in the early stage of soldering, the diffusion of Cu and Sn atoms is insufficient. Additionally, the addition of Bi and In elements prevents the interfacial IMC from selecting the orthogonal preferred orientation of (001)-oriented single-crystal copper, leading to the existence of an initial low-surface-energy scalloped morphology. As reflow time increases, the atoms diffuse more fully. Cu atoms preferentially diffuse along orthogonal directions, driving the gradual transformation of interfacial IMC into a prismatic morphology. At longer reflow times, the thickened IMC layer increases the diffusion path of Cu atoms. The addition of Bi elements disrupts the directional growth of the IMC, lowering the system's surface energy and prompting the IMC to transform from a prismatic to a scalloped morphology. Under the same reflow time, the interfacial IMC grains at 285°C are larger, with a greater number of prismatic grains, more prominent prismatic morphology, and more clearly defined 90° intergranular angles.

On (111)-oriented single-crystal copper pads, the interfacial IMC exhibits a ridged morphology. This feature becomes more pronounced with increasing reflow time, accompanied by a gradual increase in the average thickness of the Cu_6Sn_5 layer. The formation of this morphology is closely related to the densely packed (111) plane, which imposes strong directionality on Cu diffusion and promotes the preferential growth of Cu_6Sn_5 along specific crystallographic directions. Under identical reflow time, higher reflow temperatures result in larger interfacial IMC grains, a greater number of prismatic grains, and a more prominent prismatic morphology. In addition, the apex angles of the roof-ridge structures tend to approach 120°, which can be attributed to the symmetry of equivalent crystallographic directions in the Cu_6Sn_5 structure.

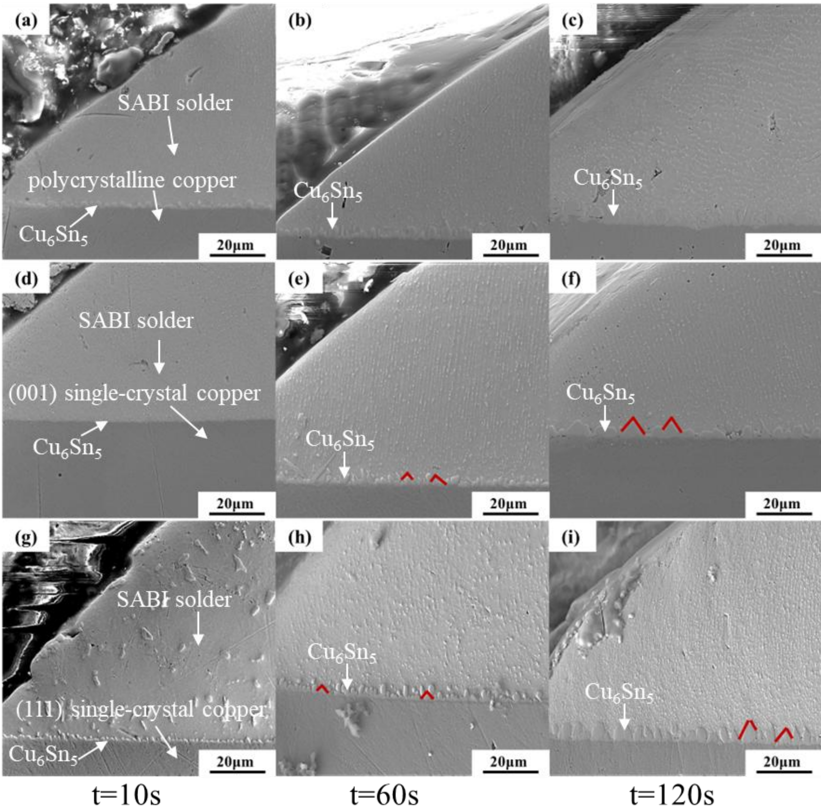

Fig. 6 Cross-sectional morphologies of interfacial IMCs formed between Sn3.5Ag0.5Bi8In solder and polycrystalline copper (a-c), (001) single-crystal copper (d-f), and (111) single-crystal copper (g-i) at 260 °C under different reflow times

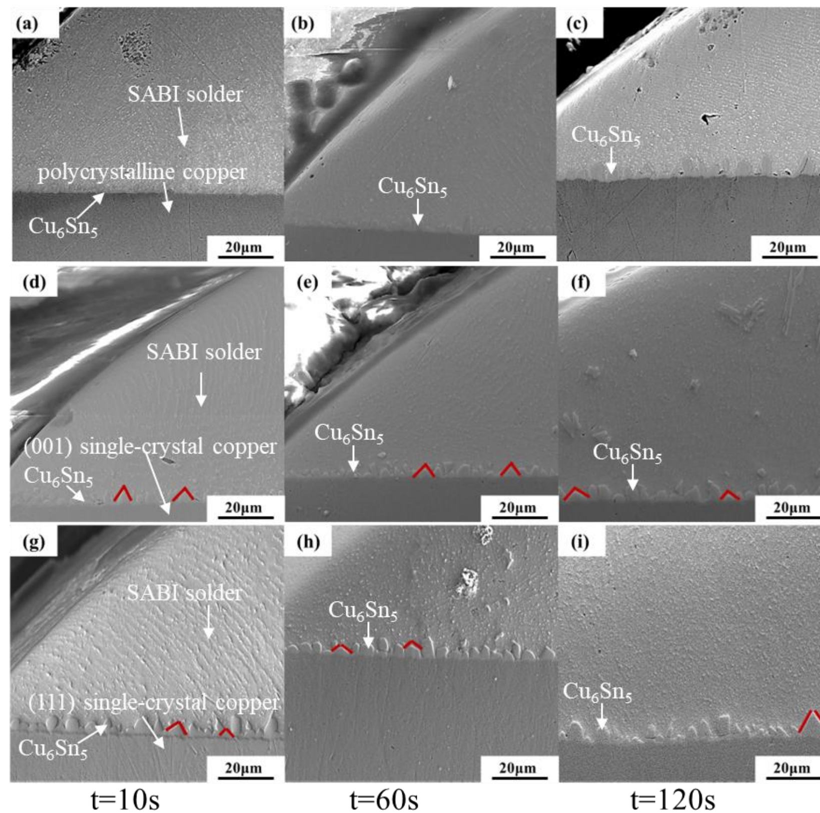

Fig. 7 Cross-sectional morphologies of interfacial IMCs formed between Sn3.5Ag0.5Bi8In solder and polycrystalline copper (a-c), (001) single-crystal copper (d-f), and (111) single-crystal copper (g-i) at 285 °C under different reflow times

3.3 Interfacial Reactions of SABI Solder with Polycrystalline Copper and Single-Crystal Copper during the aging process

An aging treatment was conducted on SABI/polycrystalline Cu solder joints that were reflowed at 260 °C for 60 s for 5, 10, 20, and 40 days. The top-view interfacial morphologies of the IMCs are shown in Fig. 8, revealing the following evolution: In the early aging stage, Cu_6Sn_5 grains exhibited a scalloped morphology. As aging time prolonged, the Cu_6Sn_5 grains flattened and transformed into a lamellar structure, with grain boundaries transitioning from clear to blurred and grain sizes continuously increasing. This is because, although the aging process lacks the high temperature of reflow, Cu and Sn atoms undergo slow solid-state diffusion during long-term isothermal holding. While the initial scalloped Cu_6Sn_5 has relatively low surface energy, local energy fluctuations drive atomic migration toward lower-energy regions, gradually flattening the "raised surfaces" of the scalloped grains. Ultimately, a more stable lamellar structure is formed, with interfacial energy far lower than that of curved surfaces. In addition, significant grain coarsening occurs during aging. Smaller Cu_6Sn_5 grains, which possess higher specific surface area and interfacial energy, tend to dissolve preferentially. Their atoms diffuse via grain boundaries or interfaces toward larger grains, thereby promoting the further growth of these grains. This process aligns with the typical Ostwald ripening mechanism: as smaller grains progressively vanish and larger grains continue to grow, the interfacial grains coarsen progressively, and the grain boundaries become increasingly indistinct due to atomic diffusion and grain coalescence.

In the cross-sectional direction of the convex point, the thickness of interfacial Cu_6Sn_5 continuously increases with prolonged aging time, gradually flattening from an uneven scalloped morphology. A large number of Cu_6Sn_5 grains are observed in the middle of the convex point, and a Cu_3Sn layer grows at the interface between the solder and the copper substrate. This is mainly because, during solid-state aging, Cu atoms continue to diffuse toward the solder along the interface and IMC grain boundaries, where they react

with Sn atoms, leading to continuous thickening of the Cu_6Sn_5 layer. With prolonged aging, the Cu_6Sn_5 phase adjacent to the Cu substrate further reacts with Cu to form the thermodynamically more stable Cu_3Sn phase, resulting in the formation of a Cu_3Sn layer between the Cu_6Sn_5 and the Cu substrate. Furthermore, Bi tends to segregate near the IMC interface during aging. This segregation reduces the diffusion rates of Cu and Sn atoms, thereby slowing the growth of interfacial IMCs and leading to a more gradual, stable morphological evolution. This indicates that the addition of Bi effectively inhibits the excessive growth of the interfacial IMC, thereby enhancing interfacial stability in the solder joint during long-term service.

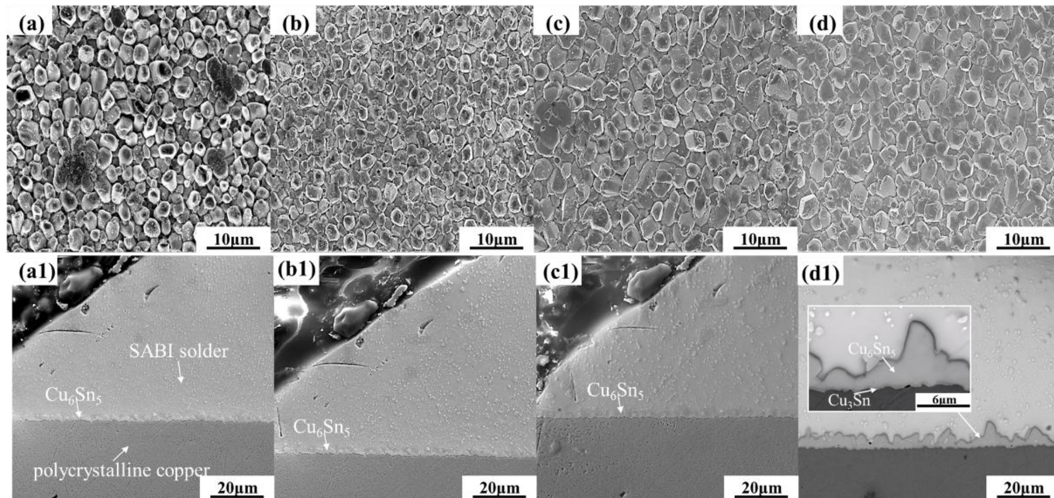

Fig. 8 Microstructural morphologies of the interface and cross-section of Sn3.5Ag0.5Bi8In solder joints with polycrystalline copper (fabricated at 260℃ for 60 s) after aging for different durations: (a) 5 days; (b) 10 days; (c) 20 days; (d) 40 days

Similarly, aging treatments were conducted on SABI solder joints on (001) and (111) single-crystal Cu substrates under the same reflow conditions (260 °C, 60 s). The corresponding top-view interfacial morphologies are shown in Fig. 9 and Fig. 10. The observations reveal that the aging behavior of a single-crystal copper convex point is similar to that of a polycrystalline one. In the early aging stage, Cu_6Sn_5 grains exhibit a scalloped morphology. As aging time increases, the Cu_6Sn_5 grains flatten and transform into a lamellar structure, with grain boundaries transitioning from distinct to blurred and grain sizes increasing continuously.

However, there are key differences: as aging time increases, prismatic grains gradually transform into scalloped grains, and the planarization time is shorter than that of polycrystalline copper convex point. In addition, the thickness of the interfacial IMC layer in single-crystal Cu joints increases more significantly with aging time and is consistently greater than that in polycrystalline Cu joints. This is because the absence of grain boundaries in the single-crystal copper substrate allows Cu atoms to diffuse freely along the crystal lattice. Compared to polycrystalline copper, the Cu_6Sn_5 layer in single-crystal copper facilitates directional diffusion along specific crystallographic orientations, thereby accelerating IMC growth. The diffusion rate of Cu within the interfacial IMC layer is significantly higher than that of Sn atoms, resulting in a diffusion imbalance. Consequently, Sn atoms cannot fully compensate for the vacancies left by the outward diffusion of Cu atoms, ultimately leading to the formation of Kirkendall voids at the interface between the Cu substrate and the IMC layer.

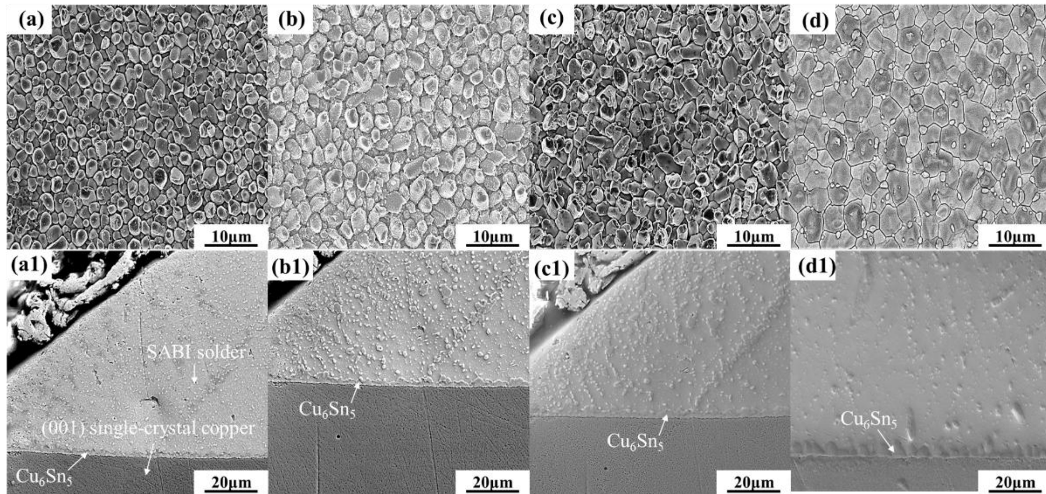

Fig. 9 Microstructural morphologies of the interface and cross-section of Sn3.5Ag0.5Bi8In solder joints with (001)-oriented single-crystal copper (fabricated at 260℃ for 60 s) after aging for different durations: (a) 5 days; (b) 10 days; (c) 20 days; (d) 40 days

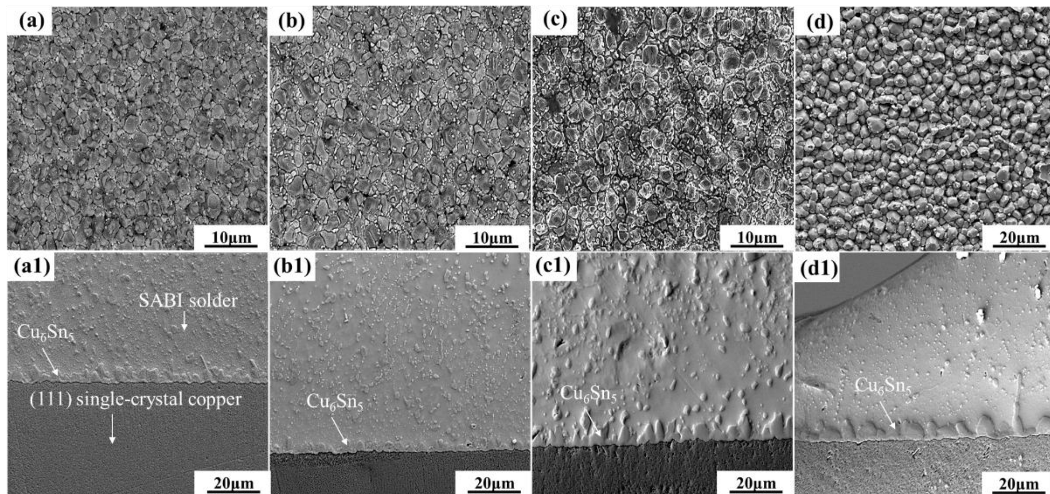

Fig. 10 Microstructural morphologies of the interface and cross-section of Sn3.5Ag0.5Bi8In solder joints with (111)-oriented single-crystal copper (fabricated at 260℃ for 60 s) after aging for different durations: (a) 5 days; (b) 10 days; (c) 20 days; (d) 40 days

3.4 Interfacial Reactions of SAC305 Solder with Polycrystalline Copper and Single-Crystal Copper during the aging process

Aging treatments were conducted on SAC305 solder joints fabricated at 260 °C for 60 s on polycrystalline copper as well as (001) and (111) single-crystal copper convex points. The interfacial IMCs morphologies are shown in Fig. 11 – Fig. 13. In the early stage of aging, Cu_6Sn_5 grains at the interface of the SAC305 solder on the polycrystalline copper exhibited a scalloped morphology in the top-view observation. As aging time prolonged, the interfacial Cu_6Sn_5 grains planarized and transformed into a lamellar structure, with grain boundaries transitioning from distinct to blurred and grain sizes continuously increasing. In the cross-sectional view, the thickness of interfacial IMC increased continuously with prolonged aging, gradually flattening from an uneven scalloped shape. A large number of Cu_6Sn_5 grains emerged in the middle of the convex point, while a Cu_3Sn layer gradually formed at the solder/Cu interface.

Compared with SABI solder in the previous section, the grains in SAC305 solder are more prone to planarization. Overall, the planarization time is shorter, and the disappearance of grain boundaries is more

obvious. This is because of the absence of Bi and In in the SAC305 solder. Bi can suppress atomic diffusion and grain growth by forming a diffusion barrier, whereas In tends to retard grain coarsening through microstructural refinement. As a result, Cu and Sn atoms in SAC305 undergo solid-state diffusion more readily, leading to accelerated grain growth and more rapid evolution of the interfacial IMC.

The aging behavior of SAC305 solder on single-crystal copper substrates was generally similar to that observed on polycrystalline copper. At an early stage, interfacial Cu_6Sn_5 grains exhibit a scalloped morphology in top view. As aging time increases, the Cu_6Sn_5 grains flatten and transform into a lamellar structure, with grain boundaries transitioning from distinct to blurred and grain sizes increasing continuously. Notably, there are key differences. The prismatic grains gradually transform into scalloped grains, and the planarization time is shorter than that of polycrystalline copper convex point during aging. This suggests that the crystallographic orientation of single-crystal copper strongly influences IMC growth behavior.

Additionally, in the cross-sectional direction, the thickness of the interfacial IMC on single-crystal copper increased with aging time and was greater than that on polycrystalline copper. This is because the absence of grain boundaries in single-crystal substrates facilitates rapid Cu atom diffusion along the lattice, thereby accelerating IMC growth. Furthermore, Kirkendall voids were observed within the interfacial IMC layer during aging, arising from the imbalance in the diffusion rates of Cu and Sn atoms.

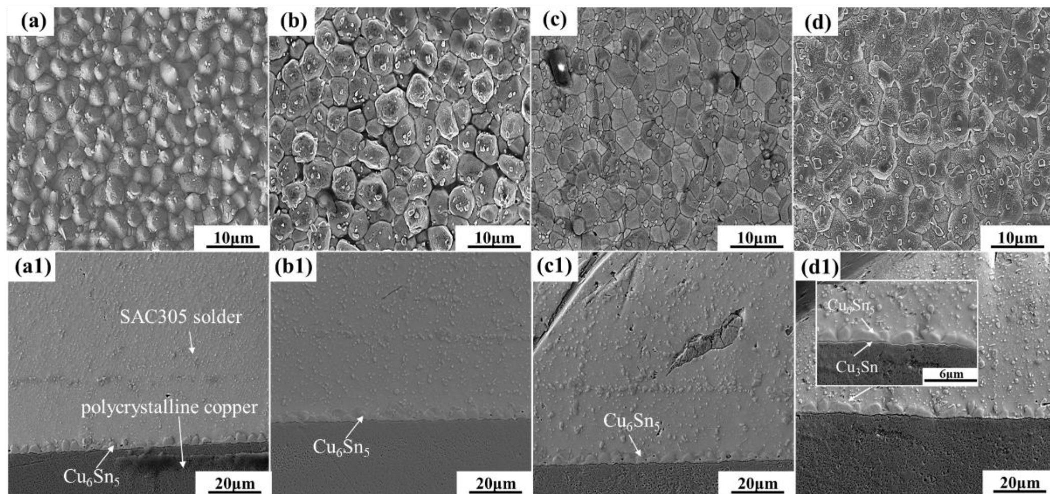

Fig. 11 Microstructural morphologies of the interface and cross-section of Sn3Ag0.5Cu solder joints with polycrystalline copper (fabricated at 260°C for 60 s) after aging for different durations: (a) 5 days; (b) 10 days; (c) 20 days; (d) 40 days

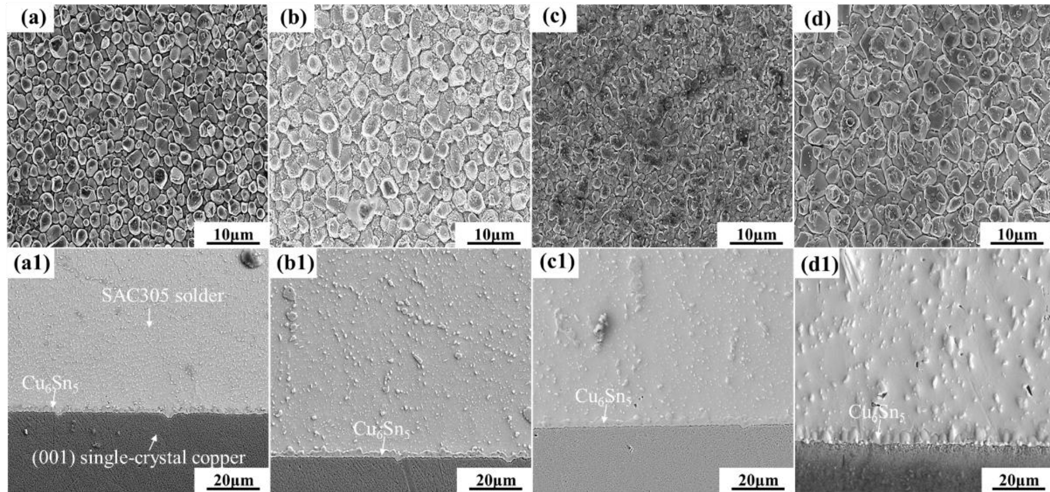

Fig. 12 Microstructural morphologies of the interface and cross-section of Sn3Ag0.5Cu solder joints with (001)-oriented single-crystal copper (fabricated at 260℃ for 60 s) after aging for different durations: (a) 5 days; (b) 10 days; (c) 20 days; (d) 40 days

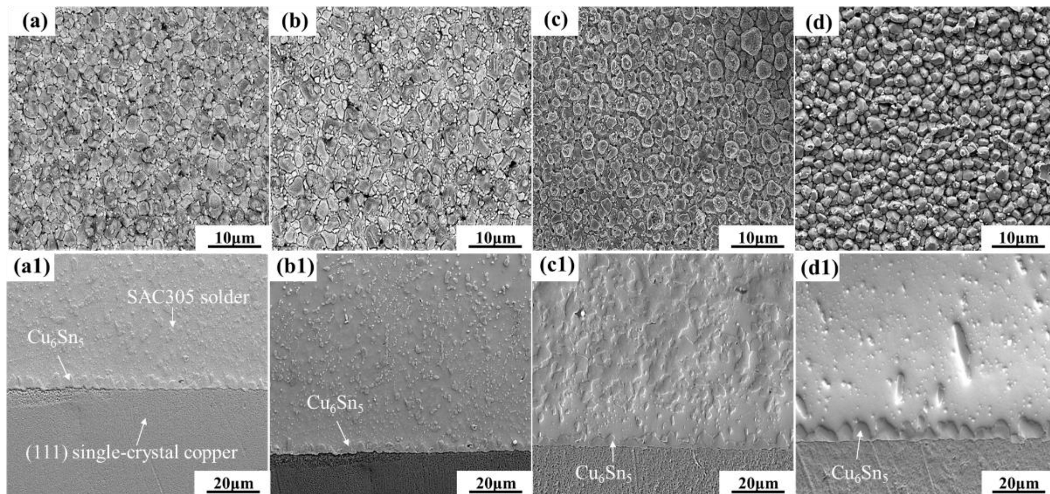

Fig. 13 Microstructural morphologies of the interface and cross-section of Sn3Ag0.5Cu solder joints with (111)-oriented single-crystal copper (fabricated at 260℃ for 60 s) after aging for different durations: (a) 5 days; (b) 10 days; (c) 20 days; (d) 40 days

3.5 EBSD Investigation on the Solder/Copper Interface Reaction

The EBSD characteristics of the cross-section of SAC305/polycrystalline copper convex-point joints, fabricated at 260℃ for 10 s, were investigated as shown in Fig. 14(a)-(d). Different colors represent the grain boundaries at different angles in Fig.(a). Among them, the grain boundaries in the solder joints are mostly small-angle grain boundaries, and a small part are large-angle grain boundaries ranging from 50° to 70°. Non-uniform diffusion plays a significant role in this behavior. During the reflow process, the diffusion rate of Cu is significantly higher than that of Sn, leading to the rapid diffusion of Cu atoms into the interfacial IMC layer. In contrast, the slower diffusion of Sn atoms limits the nucleation of Sn grains. In Fig.(b), different colors represent the crystal orientations of different Sn grains, and the shortest side of the square lattice is the C-axis of the Sn grain. By integrating the grain boundary map, misorientation distribution diagram, and pole figure of the solder joint, it is observed that Sn grains in the pole figure primarily concentrate at four positions in the solder joint. This indicates that the solder joint is polycrystalline and primarily consists of four oriented Sn grains. This phenomenon reflects the continuous interaction between Cu and Sn atoms during solid-state

diffusion, leading to multiple distinct grain orientations. Furthermore, the misorientation distribution map and pole figures visually illustrate the spatial distribution of these varying orientations, thereby reflecting the balance between the regularity and the stochastic nature of grain nucleation and growth.

The EBSD characteristics of the cross-section of SAC305/(001) single-crystal copper convex-point joints, fabricated at 260°C for 10 s, were investigated, as shown in Fig. 14(e)-(h). It can be observed that the solder joint mainly contains types of Sn grains with different orientations. Based on the grain boundary distribution map and misorientation distribution diagram, it is evident that the grain boundary angles of the two Sn grains with different orientations are all less than 15°, which are classified as low-angle grain boundaries (LAGBs). This indicates a high degree of orientational consistency within the Sn grains in the solder joint. Further analysis of the misorientation data reveals fine grains dispersed throughout the joint, suggesting they nucleated relatively quickly. The minimal orientational differences between these grains result in lower resistance to atomic diffusion, facilitating their rapid formation and growth. The pole figure of the solder joint shows two primary orientation-concentration regions, with several other scattered orientation-aggregation points. Therefore, this solder joint is polycrystalline. The LAGBs between the two dominant Sn orientations reflect a high degree of crystallographic order, resulting in a relatively regular atomic arrangement between grains. This order leads to minimal energy loss during diffusion, resulting in low resistance to diffusion at the grain boundaries.

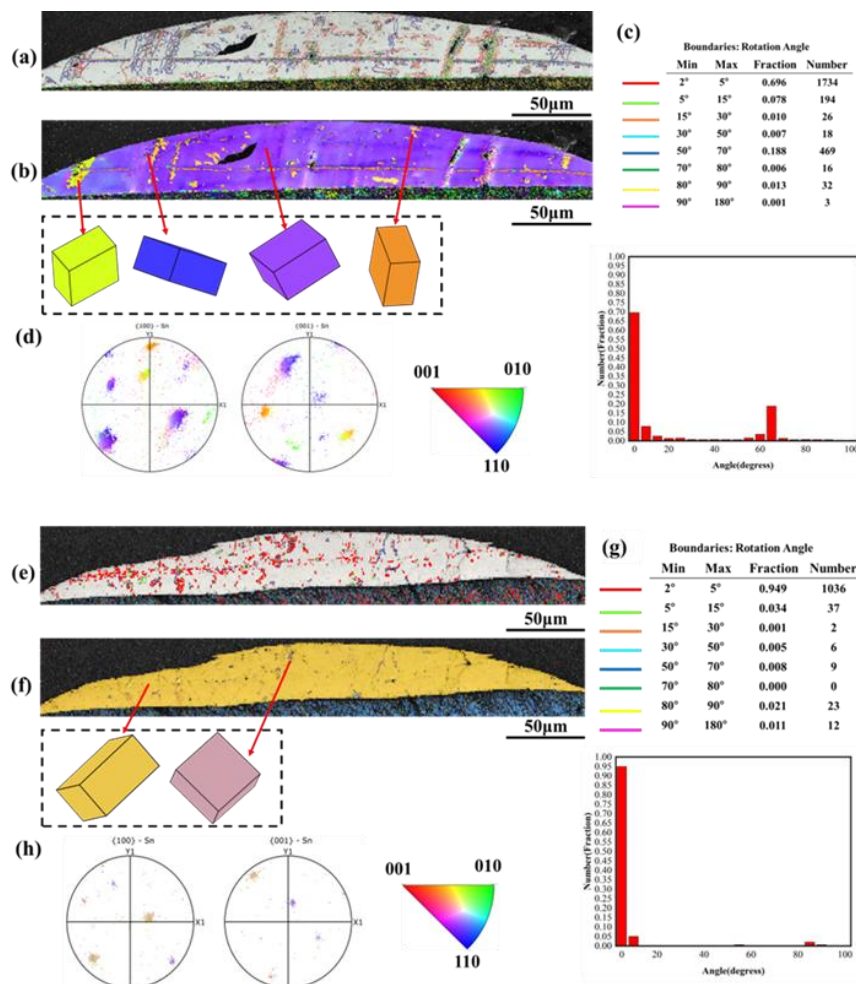

Fig. 14 Cross-sectional EBSD morphology of Sn3Ag0.5Cu Solder convex point joint on polycrystalline copper substrate(a-d) and single-crystal copper(e-h) after 10 s of Soldering at 260 °C [(a, e) Grain boundary distribution map, (b, f) Grain orientation distribution map, (c, g) Grain boundary statistical chart, (d, h) Pole figure]

The EBSD characteristics of the cross-section of SAC305/(111) single-crystal copper convex-point joints, fabricated at 260℃ for 60s, were investigated, as shown in Fig. 15. It can be observed that the solder joint mainly contains two distinct crystallographic orientations. Based on the grain boundary distribution map and misorientation distribution diagram, it reveals that the grain boundary angles between the two differently oriented Sn grains were less than 15°, indicating LAGBs, while the misorientation between the two orientation groups is approximately 60°. The presence of LAGBs indicates that adjacent grains exhibit only slight orientation differences, with relatively ordered atomic arrangements and low grain boundary energy. Such characteristics facilitate atomic diffusion along grain boundaries, thereby promoting grain growth. The joint's pole figure exhibits two distinct crystallographic orientation convergence points, which do not fuse and are distributed at two positions. This indicates that during growth, the Sn grains within the solder joint formed two sets of oriented structures exhibiting a specific symmetrical relationship. The 60° misorientation between these two groups, combined with the prevalence of LAGBs, suggests that orientation-dependent lattice rotation occurred during grain growth, leading to two sets of grains with a specific crystallographic relationship resembling mirror symmetry. Consequently, this solder joint can be identified as a twinned solder joint.

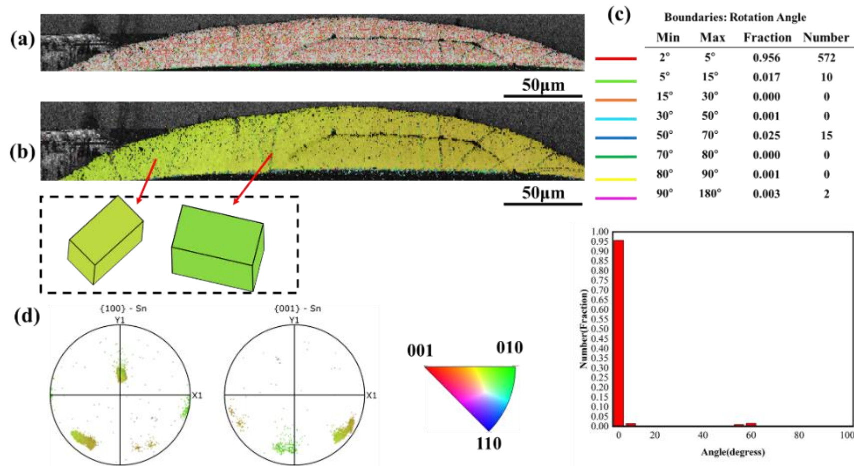

Fig. 15 Cross-sectional EBSD morphology of Sn3Ag0.5Cu solder convex point joint on (111) single-crystal copper substrate after 60 s of soldering at 260 °C (a) Grain boundary distribution map, (b) Grain orientation distribution map, (c) Grain boundary statistical chart, (d) Pole figure)

The EBSD characteristics of the cross-section of SABI/polycrystalline copper convex-point joints, fabricated at 260℃ for 60s, were investigated, as shown in Fig. 16(a)-(d). The solder joint contains Sn grains of various orientations, with several localized orientation clusters observed. This indicates that the grains underwent multi-site nucleation and random growth. The addition of Bi and In elements further influenced the distribution of grain orientations. Bi typically inhibits the growth of Sn grains, thereby promoting greater diversity in grain orientations, while In facilitates grain nucleation at multiple sites by regulating Sn diffusion, thereby intensifying the random growth of grains. Ultimately, the combined effects of these factors result in the solder joint exhibiting a typical polycrystalline structure.

The EBSD characteristics of the cross-section of SABI/(001) single-crystal copper convex-point joints, fabricated at 260℃ for 60s, were investigated, as shown in Fig. 16(e)-(h). The results indicate that the grain boundaries within the solder joints are dominated by LAGBs, with only a small fraction of high-angle grain boundaries (HAGBs) ranging from 50° to 70°, suggesting that the orientation difference between Sn grains is small and the atomic arrangement is highly ordered. Furthermore, analysis of the orientation map and pole figure reveals that the solder joints are polycrystalline, mainly composed of Sn grains with two dominant orientations, along with a sparse dispersion of fine grains with other orientations. The misorientation between the two dominant orientations is below 15°, classifying them as LAGBs, which suggests a tendency toward

orientation alignment and a relatively stable interfacial structure. These characteristics demonstrate that, under the orientational constraint imposed by the (001) single-crystal copper substrate, the Sn grains underwent preferential growth.

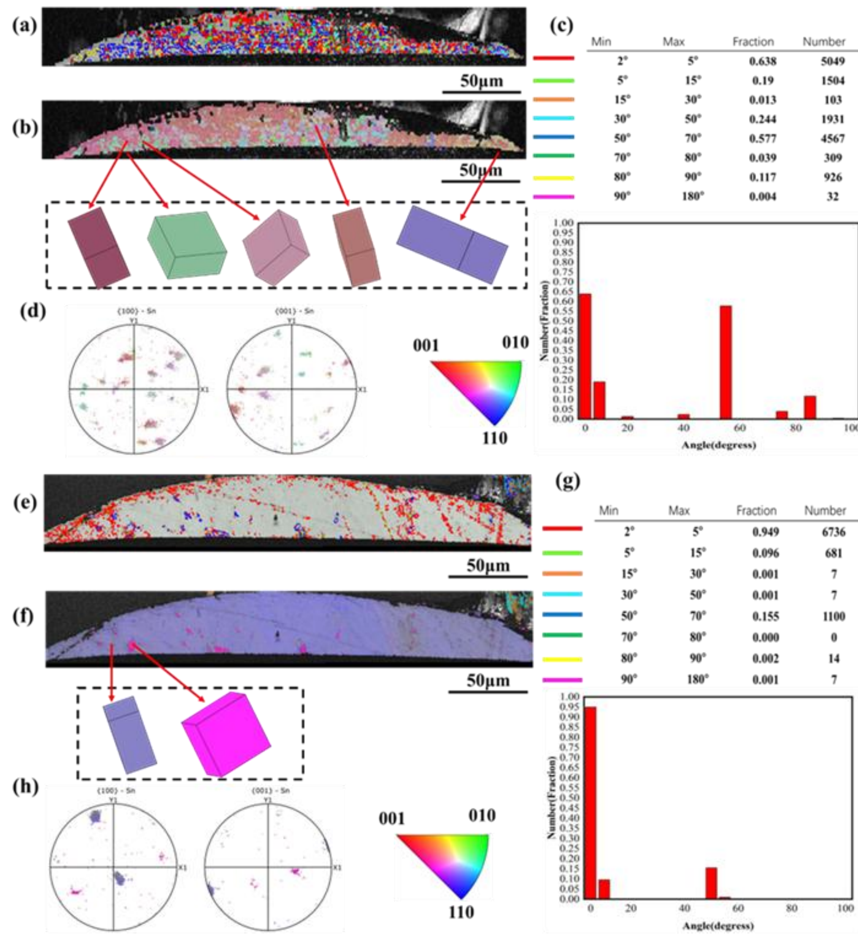

Fig. 16 Cross-sectional EBSD morphology of Sn3.5Ag0.5Bi8In solder convex point joint on polycrystalline copper substrate(a-d) and single-crystal copper(e-h) after 10 s of Soldering at 260 °C [(a) Grain boundary distribution map, (b) Grain orientation distribution map, (c) Grain boundary statistical chart, (d) Pole figure]

The IMC EBSD characteristics of interfacial IMC of SABI, SAC305/(111) single-crystal copper convex-point joints, fabricated at 260°C for 60 s, were investigated, as shown in Fig. 17. The EBSD results show that the roof-shaped Cu_6Sn_5 formed on the single-crystal copper has basically the same orientation with only slight rotation, thereby presenting different crystal structures. By comparing the EBSD results, it can be observed that, unlike SAC305 solder, which is more likely to form single-crystal or twinned solder joints, SABI solder joints are predominantly interlaced polytwinned or polycrystalline. The reason is that adding Bi and In to the SABI solder lowers the solder's melting point and increases undercooling, thereby promoting the nucleation of Sn grains. By providing a greater abundance of nucleation sites, this process ultimately results in a more complex grain structure with multi-twinned or polycrystalline characteristics.

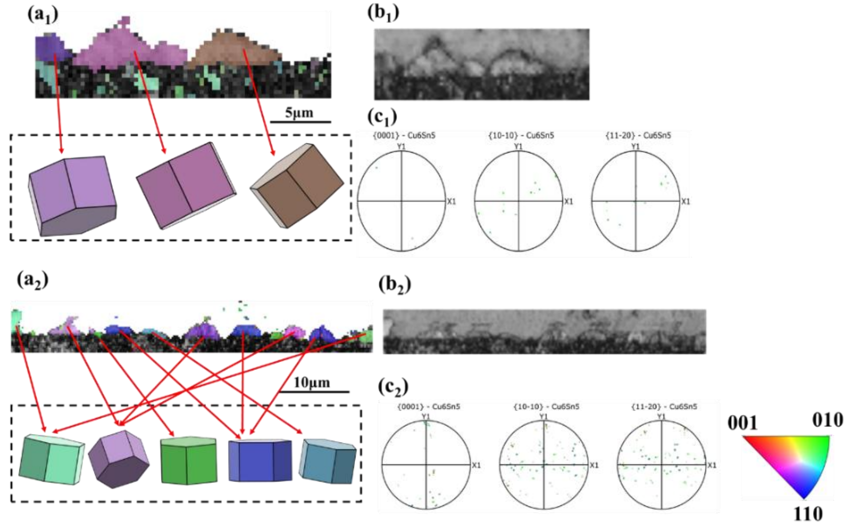

Fig. 17 EBSD analysis diagram of solder joint interface (a1, a2: IMC grain orientation of Sn3Ag0.5Cu and Sn3.5Ag0.5Bi8In solder joints; b1, b2: IMC morphology of Sn3Ag0.5Cu and Sn3.5Ag0.5Bi8In solder joints; c1, c2: IMC grain pattern of Sn3Ag0.5Cu and Sn3.5Ag0.5Bi8In solder joints)

3.6 Growth Kinetics of Interfacial IMCs during Reflow

Based on the experimental results, the IMC interface thicknesses of four combinations, namely SAC305/polycrystalline copper, SABI/polycrystalline copper, SABI/monocrystalline copper (001), and SABI/monocrystalline copper (111), at different soldering times were measured. The specific data are shown in Table. 3.

Table. 3 Interfacial IMC Thickness of Four Solder-Substrate Combinations at Different Reflow Times

IMC thickness / Welding times	SAC305 /Polycrystalline Copper	SABI /Polycrystalline Copper	SABI /(001) Single-Crystal Copper	SABI /(111) Single-Crystal Copper
10s	1.86	1.91	1.82	1.86
60s	3.45	3.98	3.81	3.93
120s	5.36	4.93	5.5	5.49

A large amount of data indicates that IMC thickness varies with reflow time according to certain kinetic laws, and that its growth is mainly controlled by lattice or grain-boundary diffusion. The following equation can express the relationship between the IMC layer thickness and time:

$$X = Dt^{n} \quad (1)$$

where X is the thickness of the IMC layer at time t (μm); D is the diffusion coefficient ($\mu m^2/s$), and D is closely related to the elemental composition of the IMC. t represents reflow or aging time (s); n is the time exponent. Transforming the above equation gives:

$$lnX = lnD + nlnt \quad (2)$$

where n is the slope of the curve ln (X_t - X_0), the value of n is as follows: if n=1/2, the growth of IMC can be regarded as lattice diffusion-controlled; if n=1/3, the IMC growth is dominated by grain boundary diffusion. If n=1, the growth of IMC can be regarded as being controlled by chemical reactions.

A linear fitting of the thickness-time relationship was conducted based on the equation, and the corresponding fitting results are shown in Fig. 18. The corresponding fitting equations are as follows:

SAC305/polycrystalline copper:

$$\ln X = 0.345\ln t - 0.17 \quad (3)$$

SABI/polycrystalline copper:

$$\ln X = 0.41\ln t - 0.30 \quad (4)$$

SABI/single crystal copper (001):

$$\ln X = 0.41\ln t - 0.35 \quad (5)$$

SABI/single crystal copper (111):

$$\ln X = 0.42\ln t - 0.35 \quad (6)$$

From the above fitting curves, the n values of the Cu_6Sn_5 phase IMC in the convex points of SAC305/polycrystalline copper, SABI/ polycrystalline copper, SABI/single crystal copper (001), and SABI/single crystal copper (111) are 0.345, 0.41, 0.41, and 0.42, respectively. All n values fall within the range of 1/3 - 1/2, indicating that a diffusion-controlled mechanism predominantly governs IMC growth in these systems.

EBSD characterization analysis reveals that the SAC305/polycrystalline copper convex point joint exhibits a high proportion of LAGBs, and LAGBs feature a highly ordered atomic arrangement. Although their diffusion capability is lower than HAGBs, due to their large quantity and the close crystal orientation of Sn grains, they remain the primary migration channels for Cu atoms. In contrast, although a small fraction of HAGBs exhibits low diffusion resistance, their low proportion results in a negligible overall impact on diffusion behavior. In addition, the aggregation of Sn grains into four preferential orientations causes the diffusion flux of Cu atoms to become directionally dispersed, thereby promoting the formation of scallop-shaped IMC morphologies at the interface. Kinetic analysis yielded a growth exponent of n = 0.345, indicating that IMC evolution in this system is primarily governed by diffusion-controlled kinetics. Combined with the EBSD observations, these results suggest that although local atomic transport is affected by the extensive distribution of LAGBs, the overall interfacial reaction mechanism remains dominated by diffusion-controlled growth.

For the SABI/polycrystalline copper convex point joint, EBSD characterization reveals a mixed distribution of LAGBs and HAGBs, with a higher proportion of HAGBs than in the SAC305/polycrystalline copper convex point joint. Owing to the low atomic packing order of HAGBs, lattice diffusion capability is enhanced. Meanwhile, the addition of Bi and In elements increases the nucleation rate, leading to more Sn grains and greater orientation dispersion, providing additional transgranular lattice-diffusion pathways for Cu atoms, thereby boosting the lattice-diffusion capacity. Although the dominant local diffusion paths differ from those in the SAC305/polycrystalline Cu joints, the calculated growth exponent (n = 0.41) still falls within the characteristic range of diffusion-controlled growth (1/3 – 1/2). Therefore, the interfacial IMC growth mechanism in the SABI/polycrystalline Cu system remains predominantly diffusion-controlled, consistent with the behavior observed in SAC305/polycrystalline Cu joints.

The EBSD analysis of the SABI/(001) single-crystal copper convex-point joint indicates that the grain boundaries within the solder joint are dominated by LAGBs, with only a small fraction of HAGBs at 50 °- 70 °. And it mainly contains two types of Sn grains with dominant crystallographic orientations, along with a sparse dispersion of fine grains with other orientations. The (001) single-crystal copper substrate has no grain boundaries and features a highly ordered atomic arrangement. The grain boundary diffusion channels depend only on the LAGBs within the solder joint itself. However, the multi-oriented Sn grains induced by Bi and In elements provide additional lattice diffusion pathways for Cu atoms, thereby enhancing the lattice diffusion capacity. The calculated growth exponent (n) remains within the range of 1/3–1/2, indicating that although local diffusion behavior is affected by the grain boundary characteristics and grain orientation distribution, the overall growth of the interfacial IMC layer is still dominated by diffusion-controlled kinetics.

For the interfacial IMCs in the SABI/(111) single-crystal copper system, the (111) substrate has a high atomic density and a compact atomic arrangement, which results in a high resistance to lattice diffusion. The

interfacial IMCs exhibit a prismatic, interlaced morphology, and EBSD shows that orientations are dispersed, resulting in an increased number of transgranular lattice-diffusion pathways. The (111) single-crystal copper substrate is free of grain boundaries, meaning that grain boundary diffusion only depends on intrinsic LAGBs and twin boundaries within the IMC phase itself. Furthermore, Bi element segregation is likely to occur at IMC grain boundaries, thereby inhibiting grain boundary diffusion and reducing its capability. Despite these morphological variations, the calculated growth exponent n remains consistent with that of other systems, specifically, n = 0.42, further substantiating that the overall growth of IMCs across these diverse systems remains a diffusion-controlled process.

In summary, although the morphologies of IMCs in different systems vary, manifesting as scalloped, prismatic, or ridge-like structures, the dominant growth mechanism across all systems remains diffusion-controlled. These morphological distinctions are primarily governed by factors such as the crystallographic orientation of the substrate, the distribution of grain boundaries, and the specific elemental composition of the solder alloy, rather than stemming from any fundamental difference in the underlying growth mechanism itself.

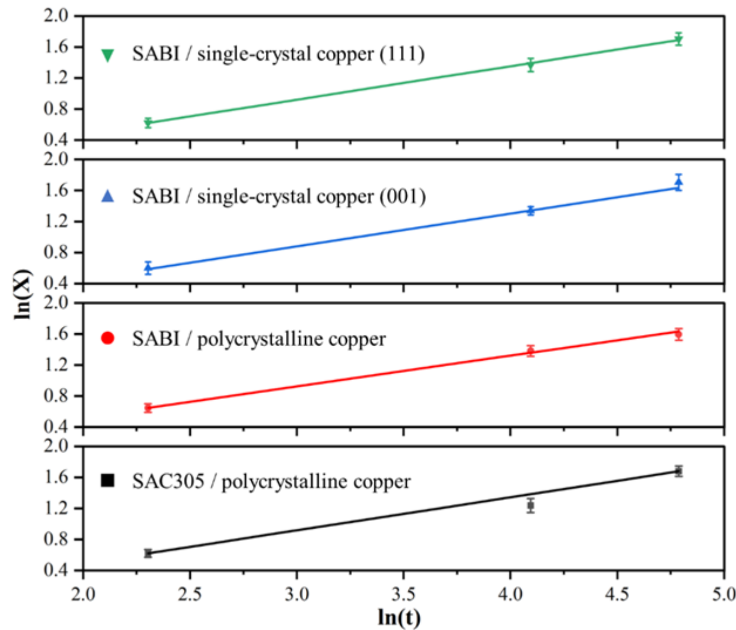

Fig. 18 Linear fitting results of the relationship between reflow time and interfacial IMC thickness for the four convex joints at 260 °C

4. Conclusions

This study systematically investigated the interfacial reaction behaviors of two solder alloys, SAC305 and SABI, during reflow and aging processes using polycrystalline copper, (001) single-crystal copper, and (111) single-crystal copper as substrate pads. The main conclusions are summarized as follows:

The crystallographic orientation of the copper substrate has a pronounced effect on the morphology of interfacial IMCs. For SAC305 solder, typical scallop-shaped Cu_6Sn_5 forms on polycrystalline copper. In contrast, regularly arranged prismatic Cu_6Sn_5 grains are observed on single-crystal substrates, with inter-grain angles of approximately 90° on (001) copper and 60° on (111) copper. With increasing soldering time, the IMC grains coarsen progressively, accompanied by a transition from scallop-shaped to prismatic morphology.

During reflow, a flower-like Ag_3(Sn, In) phase forms in the SABI solder. The interfacial Cu_6Sn_5 on single-crystal copper exhibits a ridge-like morphology, which becomes more pronounced with increasing soldering time and temperature, and subsequently transforms into a scallop-shaped structure. Compared with SAC305, this solder produces finer IMC grains, which can be attributed to the addition of Bi and In. These elements

reduce the melting temperature and promote nucleation.

During aging, the interfacial IMCs in SABI solder joints tend to form a layered structure, and the morphology evolves more rapidly toward a planar configuration, indicating improved interfacial stability. On single-crystal copper substrates, IMC planarization proceeds more quickly, and the IMC growth rate is slightly higher than on polycrystalline copper. The phase structure transformation of Cu_6Sn_5 and its relationship with the crystallographic orientation of the copper substrate will be further investigated in future work.

EBSD analysis reveals that the ridge-like Cu_6Sn_5 formed on single-crystal copper exhibits highly consistent crystallographic orientations, with only minor misorientations. Compared with SAC305 solder joints, Sn3.5Ag0.5Bi8In joints exhibit a greater tendency to form multi-twinned or polycrystalline structures.

Kinetic analysis based on reflow experiments indicates that the growth of interfacial IMC thickness follows a diffusion-controlled mechanism. In the SAC305/polycrystalline copper system, grain boundary diffusion dominates, whereas in SABI solder joints, IMC growth is governed by a combination of grain boundary diffusion and lattice diffusion. Although these diffusion modes may modify the local atomic transport pathways, the overall growth mechanism of the IMC layer remains diffusion-controlled. The evolution of IMC thickness during aging and the associated growth kinetics still need to be further investigated. In future work, a more systematic statistical analysis will be conducted to examine the evolution of IMC thickness and its kinetic behavior in detail, thereby better understanding the growth mechanism.

Experimental results indicate that the SABI solder possesses a relatively low melting point, a high nucleation rate during reflow, and good microstructural stability under complex service conditions, thereby exhibiting promising reliability performance. These findings provide useful guidance for the design of highly reliable solder joints in advanced electronic packaging and suggest considerable potential for applications in automotive electronics and high-performance electronic devices.

CRediT authorship contribution statement

Jing Han: Conceptualization, Supervision, Funding acquisition.

Hongjin Zhou: Methodology, Investigation, Formal analysis, Data curation, Validation, Writing – original draft, Visualization.

Zixuan Li: Investigation.

Chenxi Zhao: Writing – review & editing.

Zhenya Zhang: Formal analysis.

Guangming Zhang: Formal analysis, Writing – review & editing.

Fu Guo: Supervision.

Declaration of Interest

The authors declare that they have no known competing financial interests or personal relationships that could have influenced the work reported in this paper.

Acknowledgements

This work was supported by the open project of Key Laboratory of Green Fabrication and Surface Technology of Advanced Metal Materials (Anhui University of Technology) (GFST2025KF03).

References

[1] Dele-Afolabi T T, Ansari M N M, Hanim M A A, et al. Recent advances in Sn-based lead-free solder interconnects for microelectronics packaging: Materials and technologies[J]. Journal of Materials Research and Technology, 2023, 25: 4231-4263.

[2] Zhou A, Zhang Y, Ding F, et al. Research progress of hybrid bonding technology for three-dimensional integration[J]. Microelectronics Reliability, 2024, 155: 115372.
[3] Li S, Wang X, Liao M, et al. Microstructures, mechanical properties and reliability induced from size effect in Sn-based solder joints[J]. Journal of Materials Research and Technology, 2025, 35: 5067-5083.
[4] Cao J, Zhang J, Wu B, et al. Study on Manufacturing Technology of Ultra-Thin/Narrow Bonding Cu Strip for Electronic Packaging[J]. Micromachines, 2023, 14(4): 838.
[5] Wang J, Lv Z, Zhang L, et al. Nucleation and growth of Cu_6Sn_5 during the aging process of Cu/Sn interface in electronic packaging-by in-situ TEM[J]. Acta Materialia, 2024, 264: 119581.
[6] Han D G, Yoon J W. Effects of the grain size and orientation of Cu on the formation and growth behavior of intermetallic compounds in Sn-Ag-Cu solder joints[J]. Journal of Alloys and Compounds, 2025, 1010: 177801.
[7] Zhang Z, Wei H, Gao X, et al. Thermal and compositional fields to maneuver Cu_6Sn_5 intermetallic growth on (111) nanotwinned copper substrate[J]. Journal of Alloys and Compounds, 2024, 998: 174876.
[8] Xiao J, Cheng W, Fu-Kang Q. Interfacial reaction of Sn-1.5 Ag-2.0 Zn low-silver lead-free solder with oriented copper[J]. Heliyon, 2024, 10(5).
[9] Dong C, Guo T, Ma H, et al. Effect of solder composition on the growth behavior of interfacial compounds on (001) Cu and polycrystalline Cu during aging[J]. Materials Characterization, 2022, 194: 112380.
[10] Tian Y, Zhang R, Hang C, et al. Relationship between morphologies and orientations of Cu_6Sn_5 grains in Sn3.0Ag0.5Cu solder joints on different Cu pads [J]. Materials characterization, 2014, 88: 58-68.
[11] Sa Z, Wang S, Feng J, et al. Study on Cu_6Sn_5 morphology and grain orientation transition at the interface of (111) nt-Cu and liquid Sn[J]. Journal of Materials Research and Technology, 2023, 26: 9112-9126.
[12] Fazal M A, Liyana N K, Rubaiee S, et al. A critical review on performance, microstructure and corrosion resistance of Pb-free solders[J]. Measurement, 2019, 134: 897-907.
[13] Cheng S, Huang C M, Pecht M. A review of lead-free solders for electronics applications[J]. Microelectronics Reliability, 2017, 75: 77-95.
[14] Ali H E, El-Taher A M, Algarni H. Influence of bismuth addition on the physical and mechanical properties of low silver/lead-free Sn-Ag-Cu solder[J]. Materials Today Communications, 2024, 39: 109113.
[15] Zhang J, Zhang C, Pan Z, et al. Effect of Bi element on microstructure, strength and failure mechanism of Sn-Cu-In solder alloy[J]. Microelectronics Reliability, 2025, 175: 115924.
[16] Lai Y, Hu X, Li Y, et al. Influence of Bi addition on pure Sn solder joints: interfacial reaction, growth behavior and thermal behavior[J]. Journal of Wuhan University of Technology-Mater. Sci. Ed., 2019, 34(3): 668-675.
[17] Abd El-Rehim A F, Zahran H Y, AlFaify S. The mechanical and microstructural changes of Sn-Ag-Bi solders with cooling rate and Bi content variations[J]. Journal of Materials Engineering and Performance, 2018, 27(2): 344-352.
[18] Zhang H, Xu Z, Wang Y, et al. The effect of Bi addition on the electromigration properties of Sn-3.0 Ag-0.5 Cu lead-free solder[J]. Metals, 2024, 14(10): 1149.
[19] Li B, Liu S, Sun Y, et al. The effect of indium microalloying on lead-free solders: a review[J]. Materials Science in Semiconductor Processing, 2025, 185: 108956.
[20] Zhou J, Shi J, Xu L, et al. Interfacial IMC growth behavior of Sn-3Ag-3Sb-xIn solder on Cu substrate[J]. Soldering & Surface Mount Technology, 2024, 36(5): 276-284.
[21] Leal J R S, Reyes R A V, Gouveia G L, et al. Evaluation of solidification and interfacial reaction of Sn-Bi and Sn-Bi-In solder alloys in copper and nickel interfaces[J]. Metals, 2024, 14(9): 963.

[22] Ilie A A, Niculescu F, Iacob G, et al. Microstructure and properties of Bi-Sn, Bi-Sn-Sb, and Bi-Sn-Ag solder alloys for electronic applications[J]. Metals, 2025, 15(8): 915.